Supplementary material

1. Abbreviated explanation of Automatic Segmentation of Hippocampal Subfields (ASHS) algorithm/package

ASHS is a multi-atlas label fusion algorithm that propagates anatomical labels from a set of manually-labeled MRI scans called “atlases” to new unlabeled “target” MRI scans. It includes the following steps: (1) ASHS uses symmetric greedy diffeomorphic registration in the ANTs software [1] to warp each atlas to the target MRI; (2) the joint label fusion algorithm to combine the anatomical labels from the warped atlases into a single consensus segmentation in a way that assigns spatially varying weights to each atlas based on patch-level similarity to the target image while accounting for possible redundancy among the atlases [2]; (3) the corrective learning algorithm to correct for systematic segmentation biases using classifiers learned from leave-one-out segmentation of the atlas images [3]; (4) bootstrapping, i.e., using the results of multi-atlas segmentation to initialize deformable registration to improve atlas-target matching. The accuracy of ASHS relative to manual segmentation was evaluated in [4,5] using cross-validation, and shown to be comparable to the inter-rater accuracy of manual segmentation of MTL subregions.

Supplementary Table 1. Demographics and volumes of different subregions and whole hippocampus for the manual segmentations of the 7T study with controls, MCI and AD shown separately. Volumes from left and right hemispheres were averaged.

	7T dataset		
	Controls	**MCI**	**AD**
Number	19	12	7
Age (years)	70.3 (2.5)	75.2 (9.4)	75.7 (7.5)
Gender (% male)	52.6	66.7	28.6
MMSE	28.7 (1.2)	26.8 (1.9)	24.4 (2.2)
CA1 Volume	1392.4 (268.4)	1226.8 (294.3)	1186.0 (155.0)
CA2 Volume	55.0 (13.7)	51.3 (10.3)	59.7 (15.3)
CA3 Volume	115.9 (53.9)	109.8 (27.7)	93.8 (18.0)
DG Volume	760.3 (113.8)	703.3 (172.6)	580.9 (72.2)
SUB Volume	627.1 (136.5)	567.3 (116.3)	532.0 (108.5)
ERC Volume	513.4 (94.1)	483.6 (88.4)	388.7 (88.6)
Hippocampus Volume	3084.9 (495.2)	2803.5 (581.5)	2582.6 (325.9)

MCI, mild cognitive impairment; AD, Alzheimer's disease; MMSE, Mini-Mental Status Examination; CA1-3, Cornu Ammonis 1-3; DG, dentate gyrus; SUB, subiculum; ERC, entorhinal cortex; BA35/36, Brodmann Area 35/36; PHC, parahippocampal cortex

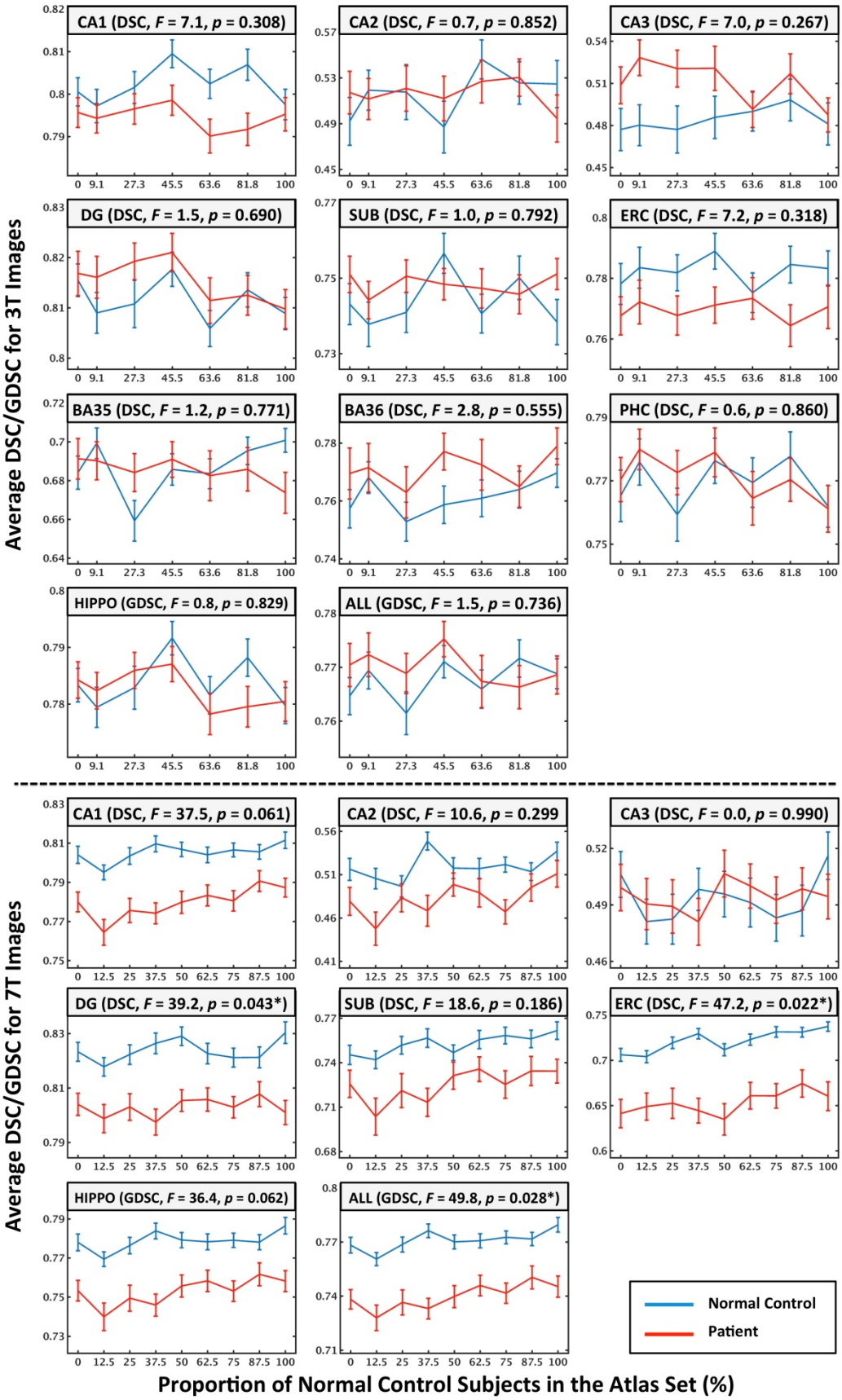
CA1 (DSC, F = 7.1, p = 0.308)
CA2 (DSC, F = 0.7, p = 0.852)
CA3 (DSC, F = 7.0, p = 0.267)
DG (DSC, F = 1.5, p = 0.690)
SUB (DSC, F = 1.0, p = 0.792)
ERC (DSC, F = 7.2, p = 0.318)
BA35 (DSC, F = 1.2, p = 0.771)
BA36 (DSC, F = 2.8, p = 0.555)
PHC (DSC, F = 0.6, p = 0.860)
HIPPO (GDSC, F = 0.8, p = 0.829)
ALL (GDSC, F = 1.5, p = 0.736)
Average DSC/GDSC for 3T Images
CA1 (DSC, F = 37.5, p = 0.061)
CA2 (DSC, F = 10.6, p = 0.299)
CA3 (DSC, F = 0.0, p = 0.990)
DG (DSC, F = 39.2, p = 0.043*)
SUB (DSC, F = 18.6, p = 0.186)
ERC (DSC, F = 47.2, p = 0.022*)
HIPPO (GDSC, F = 36.4, p = 0.062)
ALL (GDSC, F = 49.8, p = 0.028*)
Average DSC/GDSC for 7T Images
Normal Control
Patient
Proportion of Normal Control Subjects in the Atlas Set (%)

Supplementary Fig. 1. Average DSC for labels of the substructures or GDSC for the compound labels, i.e., HIPPO and ALL, versus the proportion of normal control subjects in the atlas set of 3T (top) and 7T images (bottom). Error bars indicate standard error of the mean. Importantly, GDSC of a compound label is generally lower than DSC of the corresponding binary label merging all the sublabels, because GDSC takes the size of each sublabel into account and thus will be negatively affected by the relatively lower DSC of the smaller sublabels. F statistics and p value (*$p < 0.05$) show whether segmentation accuracy (across all atlas compositions in the atlas set) differ between patients and controls for each label. Note that the comparison between 3T and 7T is not feasible because their segmentation protocols are different. This figure offers the zoomed-in views of each label instead of setting the y-axis to be the same (Fig. 1 in the main manuscript). HIPPO is the compound label of CA1-3, DG and SUB. ALL is the compound label of all the gray matter labels. of CA, cornu ammonis; DG, dentate gyrus; SUB, subiculum; ERC, entorhinal cortex; BA35/36, Brodmann area 35/36; PHC, parahippocampal cortex; HIPPO, hippocampus; DSC, Dice similarity coefficient; GDSC, generalized DSC.

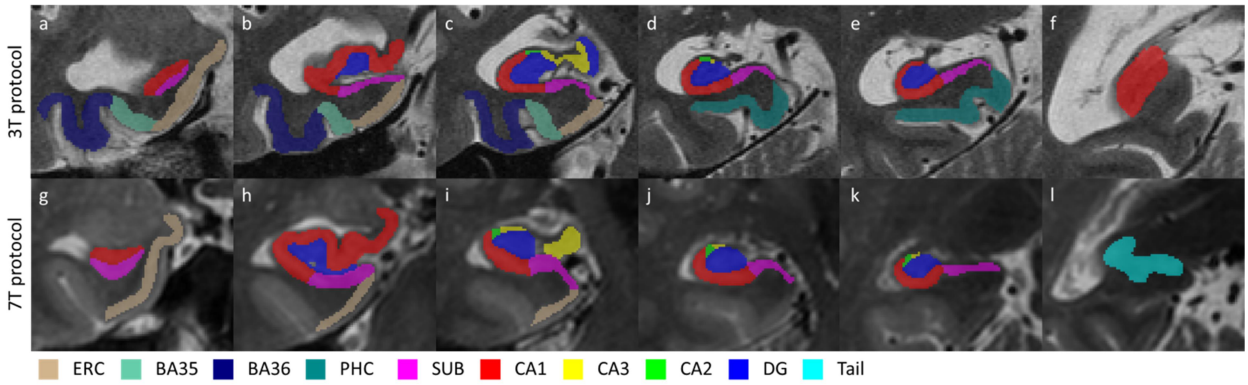

Supplementary Fig. 2. Comparison of the two segmentation protocols (3T: Yushkevich et al. [5]; 7T: Wisse et al. [6]). Images from one subject for each protocol were selected at approximately the same location along the long axis of the hippocampus. As can be seen, the protocols show similarities as well as differences. One salient difference is the location of CA2 and CA3, which is more lateral in the 7T protocol (i, j, k) and more medial in the 3T protocol (c, d). Additionally, while the subfield segmentation covers the full axis of the hippocampus in the 3T protocol (e, f), CA2 and 3 are grouped with CA1 in posterior slices (e), while in the 7T protocol the 'body protocol' as in j is used (see k) until the fornix is visible in its full extent, after which the subfields are not separated and the remaining structure receives a 'tail' label (l). Similarities can also be observed, such as the separation of the anterior portion of the hippocampus in CA1 and SUB, with CA1 covering the superior part and subiculum covering the inferior part (a, g). Other examples are the medial border of the SUB (b and h through e and k) and the similar separation of the hippocampal body into SUB, DG and CA1 (d and j, e and k), except for the border with CA2. ERC, entorhinal cortex; BA, Brodmann area; PHC, parahippocampal cortex; SUB, subiculum; CA, cornu ammonis; DG, dentate gyrus.

References:

[1] Avants BB, Epstein CL, Grossman M, Gee JC (2008) Symmetric diffeomorphic image registration with cross-correlation: evaluating automated labeling of elderly and neurodegenerative brain. *Med Image Anal* **12**, 26–41.

[2] Wang H, Suh JW, Das SR, Pluta J, Craige C, Yushkevich PA (2012) Multi-atlas segmentation with joint label fusion. *IEEE Trans Pattern Anal Mach Intell* **35**, 611–623.

[3] Wang H, Das SR, Suh JW, Altinay M, Pluta J, Craige C, Avants B, Yushkevich PA (2011) A learning-based wrapper method to correct systematic errors in automatic image segmentation: consistently improved performance in hippocampus, cortex and brain segmentation. *Neuroimage* **55**, 968–985.

[4] Yushkevich PA, Wang H, Pluta J, Das SR, Craige C, Avants BB, Weiner MW, Mueller S (2010) Nearly automatic segmentation of hippocampal subfields in in vivo focal T2-weighted MRI. *Neuroimage* **53**, 1208–1224.

[5] Yushkevich PA, Pluta JB, Wang H, Xie L, Ding S, Gertje EC, Mancuso L, Kliot D, Das SR, Wolk DA (2015) Automated volumetry and regional thickness analysis of hippocampal subfields and medial temporal cortical structures in mild cognitive impairment. *Hum Brain Mapp* **36**, 258–287.

[6] Wisse LEM, Gerritsen L, Zwanenburg JJM, Kuijf HJ, Luijten PR, Biessels GJ, Geerlings MI (2012) Subfields of the hippocampal formation at 7T MRI: In vivo volumetric assessment. *Neuroimage* **61**, 1043-1049.